20. At different temperatures, for example, synthetic rutile accommodates nonstoichiometry through different types of defects, including vacancies, crystallographic shear planes, and planar features known as platelet defects: M. G. Blanchin, L. A. Bursill, D. J. Smith, *Proc. R. Soc. London Ser. A* **391**, 351 (1984); L. A. Bursill, M. G. Blanchin, D. J. Smith, *ibid.*, p. 373.
21. Similarly, ion-exchange reactions between minerals may occur by transport through the intergranular medium, which is commonly an aqueous fluid in crustal rocks [D. M. Carmichael, *Contrib. Mineral. Petrol.* **20**, 244 (1969)]. In such reactions, dislocations and other defects may influence the kinetics of dissolution and precipitation, but they do not appear to interact structurally in the reaction mechanism [A. Baronnet, *Fortschr. Mineral.* **62**, 187 (1984)]. We therefore do not consider such dissolution-precipitation reactions further.
22. Following the usage of H. Schmalzried [*Solid State Reactions* (Verlag Chemie, Weinheim, 1981)], a reaction is solid-state if it involves solid reactants and products, even if a fluid phase is involved also as a catalyst.
23. D. R. Veblen and P. R. Buseck, *Am. Mineral.* **65**, 599 (1980).
24. J. B. Brady and R. H. McCallister, *ibid.*, **68**, 95 (1983).
25. D. R. Veblen, *ibid.* **76**, 801 (1991).
26. R. J. Angel, *ibid.* **71**, 1441 (1986); J. F. Banfield and R. A. Eggleton, *Clays Clay Minerals* **36**, 47 (1988); J. F. Banfield, D. R. Veblen, B. F. Jones, *Contrib. Mineral. Petrol.* **106**, 110 (1990).
27. S. Iijima, *J. Solid State Chem.* **14**, 52.
28. R. J. D. Tilley, *Defect Crystal Chemistry and Its Applications* (Blackie, Glasgow, 1987).
29. J. W. Christian, *The Theory of Transformations in Metals and Alloys, Part I: Equilibrium and General Kinetic Theory* (Pergamon, Oxford, ed. 2, 1975).
30. P. W. McMillan, *Glass-Ceramics* (Academic Press, New York, ed. 2, 1979).
31. G. L. Nord, Jr., A. H. Heuer, J. S. Lally, in (*4*), pp. 220–227.
32. C. Willaime, W. L. Brown, M. Gandais, in (*4*), pp. 248–257; T. L. Grove, *Contrib. Mineral. Petrol.* **64**, 273 (1977).
33. For review, see R. A. Yund, in *Feldspar Mineralogy*, P. H. Ribbe, Ed. (*Rev. Mineral.* **2**, Mineralogical Society of America, Washington, DC, ed. 2, 1983), pp. 177–202.
34. K. J. T. Livi and D. R. Veblen, *Am. Mineral.* **74**, 1070 (1989).
35. P. Robinson, M. Ross, G. L. Nord, Jr., J. R. Smyth, H. W. Jaffe, *ibid.* **62**, 857 (1977); K. J. T. Livi, *Contrib. Mineral. Petrol.* **96**, 371 (1987).
36. M. Ross, J. J. Papike, K. W. Shaw, *Mineral. Soc. Am. Spec. Pap.* **2**, 275 (1969); for review, see P. Robinson *et al.*, in *Amphiboles—Petrology and Experimental Phase Relations*, D. R. Veblen and P. H. Ribbe, Eds. (*Rev. Mineral.* **9B**, Mineralogical Society of America, Washington, DC, 1982), pp. 1–227.
37. E. A. Smelik and D. R. Veblen, *Science* **257**, 1669 (1992).
38. E. A. Smelik, M. W. Nyman, D. R. Veblen, *Am. Mineral.* **76**, 1184 (1991); E. A. Smelik and D. R. Veblen, *ibid.* **78**, 511 (1993).
39. Y.-H. Shau, D. R. Peacor, S. Ghose, P. P. Phakey, *ibid.* **78**, 96 (1993).
40. Amphiboles are classified according to the occupancy of the *M4* crystallographic site as ferromagnesian (*M4* = Fe, Mg, and Mn), sodic (*M4* = Na), calcic (*M4* = Ca), or sodic-calcic (*M4* = Na and Ca) [B. E. Leake, *ibid.* **63**, 1023 (1978)].
41. E. A. Smelik and D. R. Veblen, *ibid.* **76**, 971 (1991); *Contrib. Mineral. Petrol.* **112**, 178 (1992).
42. J. Laird and A. L. Albee, *Am. J. Sci.* **281**, 127 (1981).
43. E. A. Smelik and D. R. Veblen, in preparation.
44. Compositions of fluids in inclusions are commonly estimated from freezing and homogenization temperatures obtained with light microscopes [E. Roedder, *Fluid Inclusions* (*Rev. Mineral.* **12**, Mineralogical Society of America, Washington, DC, 1984)].
45. O. Navon, I. D. Hutcheon, G. R. Rossman, G. J. Wasserburg, *Nature* **335**, 784 (1988).
46. G. D. Guthrie, Jr., D. R. Veblen, O. Navon, G. R. Rossman, *Earth Planet. Sci. Lett.* **105**, 1 (1991).
47. G. D. Guthrie, Jr., and D. R. Veblen, *Contrib. Mineral. Petrol.* **108**, 298 (1992).
48. K. Yagi, in *High-Resolution Transmission Electron Microscopy*, P. R. Buseck, J. M. Cowley, L. Eyring, Eds. (Oxford Univ. Press, New York, 1988), pp. 568–606.
49. G. Van Tendeloo *et al.*, *Phase Transitions* **27**, 61 (1990); A. N. Goldstein, C. M. Echer, A. P. Alivisatos, *Science* **256**, 1425 (1992).
50. N. Shimobayashi, *Am. Mineral.* **77**, 107 (1992).
51. S. Ghose, G. Van Tendeloo, S. Amelinckx, *Science* **242**, 1539 (1988).
52. For reviews, see G. Dolino, *Phase Transitions* **21**, 59 (1990); P. J. Heaney and D. R. Veblen, *Am. Mineral.* **76**, 1018 (1991).
53. G. Van Tendeloo, J. Van Landuyt, S. Amelinckx, *Phys. Status Solidi* **33**, 723 (1976).
54. G. Dolino, J. P. Bachheimer, B. Berge, C. M. E. Zeyen, *J. Phys.* **45**, 361 (1984).
55. J. D. C. McConnell, *Am. Mineral.* **68**, 1 (1983); H. Böhm, *ibid.*, p. 11; J. M. Cowley, J. B. Cohen, M. B. Salamon, B. J. Wuensch, Ed., *Modulated Structures—1979* (American Institute of Physics, New York, 1979).
56. J. P. Jamet, *Phase Transitions* **11**, 335 (1988).
57. I. Hatta, M. Matsuura, H. Yao, K. Gouhara, N. Kato, *Thermochim. Acta* **88**, 143 (1985).
58. G. Dolino, F. Mogeon, P. Bastie, *Phys. Status Solidi A* **107**, 559 (1988).
59. P. Lederer, G. Montambaux, J. P. Jamet, M. Chauvin, *J. Phys. Lett.* **45**, L627 (1984).
60. P. J. Heaney and D. R. Veblen, *Am. Mineral.* **76**, 1459 (1991).
61. P. R. Buseck and D. R. Veblen, *Geochim. Cosmochim. Acta* **42**, 669 (1978).
62. J. J. Papike, in *Pyroxenes*, C. T. Prewitt, Ed. (*Rev. Mineral.* **7**, Mineralogical Society of America, Washington, DC, 1980), pp. 495–525.
63. G. E. Harlow and D. R. Veblen, *Science* **251**, 652 (1991).
64. E. S. Ilton and D. R. Veblen, *Nature* **334**, 516 (1988); *Econ. Geol.*, in press.
65. E. S. Ilton, D. Earley, III, D. Morozas, D. R. Veblen, *ibid.*, **87**, 1813 (1992).
66. B. M. Bakken, M. F. Hochella, Jr., A. F. Marshall, A. M. Turner, *ibid.* **84**, 171 (1989).
67. E. S. Ilton and D. R. Veblen, in preparation.
68. P. R. Buseck and S. Iijima, *Am. Mineral.* **59**, 1 (1974).
69. K. J. Kingma, C. Meade, R. J. Hemley, H.-k. Mao, D. R. Veblen, *Science* **259**, 666 (1993).
70. Most of the work presented here was done while the authors were in the Department of Earth and Planetary Sciences, Johns Hopkins University. The research was first presented in this form as the inaugural Gabriella Donnay Lecture at the Carnegie Institution of Washington Geophysical Laboratory. G. Donnay and J. D. H. Donnay were among the first x-ray crystallographers to comprehend the power of HRTEM for solving crystallographic problems and this article is warmly dedicated to them. We thank D. J. Smith for collaboration in the study of TiO_2. The research was funded by the National Science Foundation and the Department of Energy.

Atmosphere-Surface Exchange Measurements

W. F. Dabberdt, D. H. Lenschow, T. W. Horst, P. R. Zimmerman, S. P. Oncley, A. C. Delany

The exchange of various trace species and energy at the earth's surface plays an important role in climate, ecology, and human health and welfare. Surface exchange measurements can be difficult to obtain yet are important to understand physical processes, assess environmental and global change impacts, and develop robust parameterizations of atmospheric processes. The physics and turbulent structure of the atmospheric boundary layer are reviewed as they contribute to dry surface exchange rates (fluxes). Micrometeorological, budget, and enclosure techniques used to measure or estimate surface fluxes are described, along with their respective advantages and limitations. Various measurement issues (such as site characteristics, sampling considerations, sensor attributes, and flow distortion) impact on the ability to obtain representative surface-based and airborne flux data.

There is widespread concern about the effect of anthropogenic activities on the composition of the earth's atmosphere. A major limitation in our understanding of the chemistry of the atmosphere is uncertainty over the distribution and rates of change of trace species emissions and losses at the earth's surface. Although small and difficult to quantify accurately on the local scale, these exchanges nonetheless are very significant when integrated over the larger scales. For example, distributed emissions from rural lands and oceans are as important as locally intense industrial emissions.

Surface exchange studies range in scale from investigations of specific microbial biochemistry to projections of changes in the composition of the global atmosphere. Trace gases are both emitted and absorbed at the earth's surface. The resulting fluxes are of great importance in studying the budgets of trace species—that is, their sources, sinks, transformations, and transport. These processes interact across a broad spectrum of temporal and spatial scales. Thus, for example, investigations of soil nutrient cycling (and its dependence on

The authors are with the National Center for Atmospheric Research, P.O. Box 3000, Boulder, CO 80307–3000.

changes of moisture and temperature) must deal with the uptake and release of biologically active oxides of nitrogen. Regional air pollution studies focus on the effects of the deposition of pollutants (such as O_3 and SO_2) to different crops. Investigations into the global budget of radiatively important and chemically reactive trace gases such as N_2O and CH_4 require emission fluxes from globally important biomes. Local and global estimates of surface exchange are critically dependent on accurate and representative flux measurements that can be used for specific process studies and to develop parameterizations for wider and more routine application.

One reason for the importance of near-surface exchange processes is the relative ease of transport in the lower atmosphere. The atmosphere near the earth's surface is almost always turbulent, and trace gases are rapidly diffused to (or from) the surface by irregular or random motions generated by wind shear and buoyancy forces. As a result, the lower atmosphere responds quickly to changes in surface exchange. Turbulent diffusion is many orders of magnitude larger than molecular diffusion which can be neglected beyond a few millimeters from the surface. Not considered in this discussion are so-called wet deposition losses resulting from scavenging and washout by precipitation.

Exchange processes can be measured several ways: (i) micrometeorological techniques, which measure transport in the lower part of the atmosphere; (ii) enclosure techniques, which measure changes in mean concentration within a representative sample of a surface or biome of interest; and (iii) budget techniques, which extend enclosure principles to an unconfined volume of the atmosphere. These techniques may also be classified as direct or indirect, depending on whether the flux is actually observed or estimated through parameterization methods or empirical relations.

Atmospheric Boundary Layer Structure

The atmospheric boundary layer (ABL) is the lower part of the troposphere that interacts with the biosphere and is closely coupled to the earth's surface by turbulent exchange processes. The time required to mix a constituent released at the surface throughout the ABL is typically on the order of 1 hour. The depth of the ABL (z_i) varies from a few tens of meters when the air near the surface is stably stratified (that is, the surface is colder than the air above, as typically occurs over land at night) to several kilometers when the surface is heated by the summer sun and the air is convectively unstable.

The surface layer (SL) is the lower part of the ABL where vertical fluxes of conserved quantities can be considered constant (to ~10%; the SL depth is $\sim 0.1z_i$). Although SL fluxes are nearly constant, concentrations vary approximately logarithmically with height. The relations in the SL between fluxes and vertical profiles of trace species, as well as the behavior of other turbulence statistics, are dependent on the character of the surface, as specified by a roughness (for momentum) or transfer (for trace species) length scale, the hydrodynamic stability, and the mean wind.

The commonly used measure of hydrodynamic stability in the SL is the Monin-Obukhov length (L). Monin-Obukhov similarity theory (*1–3*) is based on expressing vertical gradients and turbulent statistics of variables in the SL as functions of the ratio of height (z) above the surface to L. The dimensionless ratio ($-z/L$) is defined as the ratio of the turbulent energy produced or consumed by buoyancy to the turbulent energy generated by wind shear (where the shear is given for a neutrally stratified SL). Buoyant energy is generated by relatively light volumes of air moving upward and heavy volumes moving downward. Both temperature and water vapor contribute to the buoyancy, and their combined effect on air density is given by the virtual temperature (*4*). Although temperature is usually dominant, an exception occurs over the ocean where typically the atmosphere and ocean are at nearly the same temperature. In that case, it is possible to have a positive virtual temperature flux with the surface temperature slightly cooler than the atmosphere.

Above the SL, when the surface virtual temperature flux is positive (unstable stratification), a different similarity structure applies. In this region of the convective boundary layer (CBL), called the mixed layer (ML), z_i is the relevant height scale. This reflects the fact that the turbulent eddies predominantly effect vertical transport scale with z_i. Further, wind shear near the surface is no longer the predominant source of turbulent energy; rather, buoyancy dominates in the ML. The relevant velocity scale becomes the convective velocity, which is proportional to the cube root of the buoyancy flux (*5*), and z_i. Mixed-layer scaling depends not only on the surface fluxes but also on entrainment fluxes through the top of the ML (*6–8*).

Compared to the SL, mixing processes in the CBL are so efficient that vertical concentration gradients of conserved species are small. Here the vertical transport is dominated by thermals—buoyant plumes generated within the SL by surface heating. They extend through the CBL, mix with surrounding air, and eventually lose their momentum near the top of the boundary layer. The turbulent energy given off by impingement of these turbulent eddies on the overlying inversion entrains overlying stably stratified (warm) air into the CBL. The net result is a growing turbulent CBL that rapidly diffuses any trace constituent, whether introduced at the surface, through the top, or between. The time to uniformly mix a constituent introduced at the earth's surface ranges from minutes within a few meters of the surface to tens of minutes throughout the upper ML (*9*). Unless the lifetime of a trace species is greater than its diffusion time, then vertical profiles of its flux and mean structure will differ from that of conserved species (*10–12*). Examples of chemical reactions that can have time scales comparable with diffusion times are the NO-NO_2-O_3 triad in the SL and the reaction of isoprene with OH in the ML.

The stable boundary layer (SBL) forms over land in the evening as the ground cools; mixing is much reduced compared to the CBL, and concentrations of trace species released (or deposited) at the surface are likely to be larger (or smaller). In the classical case, turbulence is generated by shear near the surface and damped by the static stability so that the turbulence energy decreases with height in the shallower SBL. Turbulence becomes increasingly intermittent with height, with no pronounced jump in stability or reduction in turbulence across the top as happens with the CBL. The depth of the SBL can be specified as the height at which the turbulence energy is reduced to a small fraction (such as 5%) of the SL value (*13*). Typically the SBL depth is of order of several tens of meters to a few hundred meters. In the upper SBL, stable stratification gives rise to gravity waves and periodic oscillations but little or no vertical transport.

Very stable cases typically occur over land with light winds and strong surface cooling (clear skies). Here the SBL is often complex because of the interacting processes of clear-air radiative cooling, separation of flow into discrete stratified layers, intermittency of turbulence, and frequent occurrence of a low-level jet above the surface inversion layer (*1*). In this situation, boundary-layer structure cannot be predicted from the usual similarity theory (*14*). For example, if the main source of turbulence energy is at the top of the inversion layer near the low-level jet, then a consequence is an inverted boundary-layer structure.

During a typical diurnal cycle over land, the CBL grows rapidly through the morning but more slowly early in the afternoon. By late afternoon, turbulence decreases and mixing is reduced. In the evening, the ground radiatively cools below the air temperature and an SBL develops, which may grow slowly through the night. After sunrise, the CBL again forms when the ground becomes warmer than the overlying air and warms the stable layer that developed through the night. Often fair weather cumulus clouds form at the top of the CBL. If the clouds grow sufficiently they can have a significant impact on flux profiles, both through the effects of induced air circulations and modification of the surface radiation budget (*1*). The typical diurnal variation of the surface energy balance over land in the absence of clouds is illustrated in Fig. 1. The measurements were made with the Atmospheric-Surface Turbulent Exchange Research Facility (ASTER) (Fig. 2).

Over the ocean, the diurnal cycle is quite different and often scarcely noticeable. Ocean waters have a much larger effective heat capacity and conductivity, and the surface temperature is hardly perturbed by the daily solar cycle. More importantly, in clear daytime conditions boundary-layer air is heated directly by the sun, typically more than compensating for infrared cooling. In this case, the daytime ABL is more stable (smaller virtual temperature flux and less cloudiness) than the nocturnal boundary layer.

Techniques for Flux Measurement

Ambient fluxes are measured with a variety of techniques, each with its own advantages and limitations. We discuss the most important and the most common techniques: micrometeorological methods, budgets, and enclosures. However, there is no single best method for all applications; most of these techniques are complementary.

Micrometeorological techniques. The most direct micrometeorological approach to determining surface constituent exchange is the measurement of the vertical turbulent flux near the surface. The flux is the average of the instantaneous product of vertical velocity (w) and constituent density (species mass per unit volume) or mixing ratio with respect to air (species mass per mass of air). This is the eddy correlation technique. Because turbulent fluctuations are by nature irregular and random, they normally are quantified as statistical averages. The time series must be sufficiently long to ensure that the calculated averages are statistically well behaved (see discussion below).

Usually, the sample rate for digitally recording variables for eddy correlation is several times the inverse of the highest frequency of the instrument response. However, for a given level of accuracy, it is only necessary that samples be obtained about once per integral time scale (a measure of the interval over which, on average, a variable is correlated with itself) without increasing the averaging time; furthermore, the samples must be obtained rapidly—within a fraction of an integral time scale. When the concentration is multiplied by w at the time the sample is collected, short-wavelength contributions to the flux are retained. Because the flux integral scale is roughly an order of magnitude larger than the shortest significant wavelength contributing to the flux, it is possible to use chemical instruments with considerably slower response than with conventional eddy correlation. If samples are collected at a rate less than the integral scale, the flux can still be measured provided the averaging period is increased to retain the same level of accuracy. Cooper (*15*) has described and demonstrated this technique for aircraft measurements of water vapor flux.

Summertime eddy-correlation flux measurements of water vapor, carbon dioxide, ozone, and temperature over a cotton field are shown in Fig. 3. Although eddy correlation is the most direct and fundamental micrometeorological way to measure fluxes, it is not always feasible or practical and so other flux measurement techniques are often used. They are ordered below roughly to the degree that they rely on empirically determined results or assumptions.

Conditional sampling techniques collect air samples in various reservoirs as determined by some property of the vertical velocity. The eddy-accumulation technique is a conditional sampling method that does not involve empirical relations (*16*). Air is collected in two reservoirs: one when $w < 0$ and the other when $w > 0$. The volume rate at which the sample is collected is proportional to the magnitude of w. The result is that the flux of species c is estimated from the difference in mass of c collected in each reservoir divided by the collection time. Thus, fast-response concentration measurements are not required for eddy accumulation. Hicks and McMillen (*17*) and Cooper (*15*) point out that: (i) very accurate mean concentration measurements are required, as with most micrometeorological techniques; (ii) controlling the flow rate with the required speed, accuracy, and dynamic range is difficult; and (iii) it is necessary to remove mean vertical velocity offsets in real time. As a result, eddy accumulation is difficult to implement.

In many cases, however, species sensors do not have the required frequency response for direct eddy correlation so that other conditional sampling techniques have been developed. Businger and Oncley (*18*) discuss a simplification of the eddy accumulation approach. They show that if samples of up- and down-moving air are collected at the same rate in each of the reservoirs, the species flux is given by the product of the standard deviation of w, the difference in species concentration, and a scaling parameter b. This scaling parameter, which they determined to be ~ 0.6, is dependent upon the probability distribution of w. Wyngaard and Moeng (*19*) show that $b = 0.63$ for a joint Gaussian probability distribution for w and c. Furthermore, by using computer simulations of turbulence eddy structure in the

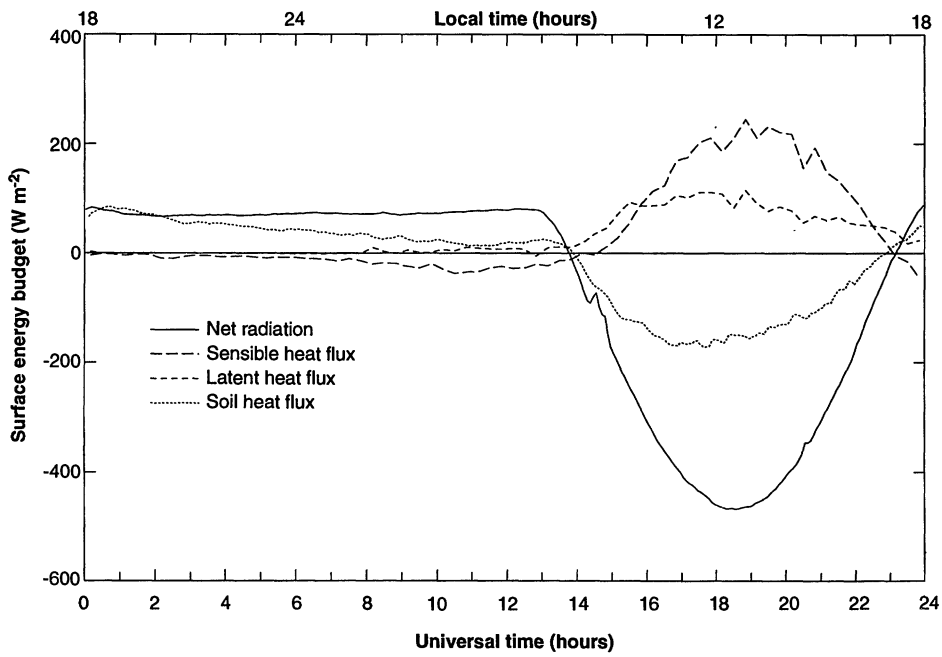

Fig. 1. Typical diurnal variation of the surface energy balance of fallow farmland under winter clear-sky conditions. The measurements were obtained with ASTER (see Fig. 2) on 28 February 1992, near Sabetha, Kansas, as part of the mesoscale STORMFEST experiment. Here, upward fluxes are denoted positive.

CBL, they found good agreement with the value $b \simeq 0.6$ for constituents with sources or sinks at the surface, but a smaller value ($b \simeq 0.47$) was found for sources or sinks above the ML. Recent applications (*20–22*) of conditional sampling for CO_2 and water vapor have been quite encouraging.

Another commonly used technique is the gradient method. In the SL, similarity theory predicts a unique relation between the flux and the vertical gradient of species concentration when the source or sink of the species is at the surface. The coefficient of proportionality, known as the eddy diffusivity, depends on stability and the stress, or momentum flux at the surface.

The gradient technique can be extended to estimate fluxes over the open sea by relating the flux of a quantity to the product of the difference in these quantities between values at the surface and some reference height (usually 10 m) and the mean velocity at the reference height. The coefficient of proportionality is known as an aerodynamic or bulk transfer coefficient. Thus the fluxes of temperature and humidity can be estimated by measuring surface temperature as well as the mean wind, air temperature, and humidity at 10 m (*23*).

Fluxes of other trace species across the air-sea interface often are estimated from the difference between the air and water concentrations of the trace species times a transfer velocity (*24*). The transfer velocity includes contributions from transfer through both water and air. This transfer velocity may be expressed either in terms of the water concentration or the air concentration, which are related through the Henry's Law constant H, the dimensionless ratio of the equilibrium trace species concentration in air (in kilograms per cubic meter of air) to the equilibrium concentration of nonionized dissolved gas in water (in kilograms per cubic meter of water) (*24*). Neglecting chemical reactivity effects, for species with a small Henry's Law constant or that are chemically active in water, the flux is controlled by the transfer velocity through the air. Examples include H_2O, HCl, SO_2, NH_3, and HNO_3. On the other hand, for species with a large Henry's Law constant, the flux is controlled by the transfer through the water; examples include CO_2, CO, CH_4, N_2O, dimethyl sulfide (DMS), and methyl iodide (*25, 26*).

Similarly, deposition of trace species to different surfaces is often written in the form of a resistance (the reciprocal of a transfer velocity) in analogy to electrical circuitry. Examples are surface deposition for species such as O_3, SO_2, and HNO_3 that react with and are absorbed on vegetation. The resistance to deposition is expressed as:

$$r = r_a + r_s + r_c \tag{1}$$

In this context, r_a is the aerodynamic resistance of the atmosphere from a reference height z down to the roughness length z_0; r_s is the resistance across the laminar sublayer; and r_c is the remaining (residual) resistance due to the less-than-perfect absorption of molecules or particles that strike the surface (*27*). Often the deposition velocity, $v_d \equiv r^{-1}$, is used to describe the absorption of trace gases or particles at the surface by expressing the deposition flux as the product of v_d and c (at the reference height). Businger (*28*) describes limitations and accuracy of many of the techniques that measure deposition of trace constituents at the surface.

Both entrainment and surface fluxes affect the mixed layer concentration profile. Therefore, two equations and a minimum of three levels of concentration measurements are needed to obtain the surface flux. Davis (*29*) demonstrates this technique for isoprene and other hydrocarbon measurements at several levels on a tethered balloon. This technique is particularly promising for estimating fluxes where SL measurements are difficult.

Measurement of fluxes in the vicinity of a plant canopy presents added complications compared to measurements well above the canopy. The structure within the foliage does not follow the similarity laws previously discussed. Here, simple gradient diffusion models are not adequate for describing vertical transfer. Raupach (*30*) has shown, however, that vertical profiles of normalized turbulent quantities within and just above canopies tend to collapse onto universal curves normalized by the canopy height, although mean quantities also depend on canopy structure. Raupach *et al.* (*31*) also found that canopy turbulence is much more intermittent than turbulence above the canopy and exhibits characteristic coherent structures.

Apparent turbulent diffusivities just

Fig. 2. ASTER surface flux instrumentation deployed in a cotton field in the San Joaquin Valley of California. [Photo by T. Horst.] The ASTER measurement facility (*75*) was developed at NCAR to provide field measurement and data analysis support to a broad spectrum of physical scientists concerned with air-surface exchange processes. Specific scientific objectives of ASTER include documentation of atmospheric surface-layer structure in support of chemical measurements for study of dry deposition, resuspension, and chemical reactions, flux information for boundary-layer and turbulence studies, study of transfer processes to and from crops and within plant canopies, ground truth in support of remote sensing from aircraft and satellites, and field testing of new chemical and meteorological sensors. ASTER consists of three elements: (i) meteorological and chemical sensors; (ii) remote data-acquisition and telemetry modules; and (iii) central data processing, analysis, display and archival system. Meteorological sensors include fast-response one- and three-dimensional sonic anemometers, ultraviolet (UV) hygrometers, platinum resistance thermometers, slow-response propeller-vane anemometers, psychrometers, pressure sensors, rain gauges, surface-energy balance (radiation and heat) sensors, and special radiation sensors (UV radiometers and PAR radiometers). Available chemical sensors are condensation nuclei counter, CO analyzer, O_3 analyzer, fast SF_6 analyzer, and conditional-intermittent samplers. The system is designed to easily integrate special sensors. Six aerodynamically slender, 10-m towers each support flux and profile instrumentation according to the experimental design; user towers may also be used. ASTER data-acquisition modules (ADAMs) are the interface between the sensor arrays and the field base station. The ADAMs operate in a real-time mode to sample and process analog and digital data from conventional sensors and assimilate serial data from integrated or intelligent sensors. They format the data and transfer message streams to the base station. Two-way communication exists between each ADAM and the base station using a fiber optic cable, enabling dynamic control of sampling protocols. Interface cards provide 8 serial communication channels and 48 14-bit analog channels with front-end amplification and filtering as needed. A typical ADAM data rate is 320 samples per second in analog mode plus 3600 characters per second serial mode. Burst-mode sampling supports 8-kHz data rates on a single channel on each ADAM. The base station and field instrumentation laboratory are housed in a linked pair of redesigned 6-m seatainers. The base station is a general-purpose computing facility that provides data acquisition, archive, analysis, and display functions. Routine processing includes archival of all raw data, data monitoring, and continuous calculation of moments, covariances, and other statistics.

above the canopy (in the so-called roughness sublayer) can be as much as two to three times those predicted from classical theory. One approach is to measure above the roughness sublayer, whose depth is estimated to be about three to four times the scale of the horizontal inhomogeneities in the canopy (*32, 33*). This may often be inconvenient or undesirable because concentration differences are smaller and fetch requirements are greater at the higher levels. For this reason, Cellier and Brunet (*33*) have devised generalized flux-profile relations applicable within the roughness sublayer.

A further complication is the difference in diffusivities for different species that may occur just above the canopy depending upon their sources or sinks. For example, during daytime, isoprene is emitted by leaves while N_2O is emitted at the ground. Quantifying these diffusivity differences is an area that requires further research.

Another approach to measuring surface fluxes is to utilize the surface energy budget to evaluate the sensible heat flux (temperature flux times the specific heat at constant pressure) and the latent heat flux (humidity flux times the latent heat of evaporation). Over land, the sum of these fluxes equals the net radiation R_n at the surface minus the soil heat flux G in the absence of heat storage and release by a canopy. Assuming that the transfer characteristics and the distribution of surface sources and sinks for temperature, humidity, and a trace species are identical, the flux of a trace species is equal to the ratio of (R_n − G) to the mean difference in total (sensible plus latent) heat between two levels times the mean difference in species concentration between the same two levels (*1, 34, 35*). Advantages of this approach are that eddy flux measurements and stability corrections are not required; a drawback is that it requires measurements of R_n and G. A further drawback is the difficulty in measuring canopy heat storage and release.

Alternatively, a trace species flux can be estimated from measurements of the flux of some other scalar such as temperature or humidity times the ratio of the difference in concentration to the difference in the other scalar. Instead of the ratio of mean differences, the ratio of standard deviations may also be used, although the sign of the flux is not preserved. This technique may be particularly useful in situations such as estimating fluxes over forests where SL similarity relations are difficult to apply. Again, with all techniques that use a surrogate variable to characterize the transport process for species concentration, it is assumed that the transport process and the distribution of sources and sinks are identical for the two variables.

Another approach to estimating fluxes is to use turbulence moments, which can be related to surface fluxes through the similarity relations discussed previously [for example, (*36*)]. A straightforward example estimates the magnitude of the surface flux from the standard deviation of fluctuations in species concentration. (This approach uses the fact that surface fluxes normally are the source of concentration fluctuations; the method can be used both in the SL and ML. The sign of the flux must be determined independently.)

A related approach is the dissipation technique, which is based on the hypothesis that the dissipation of turbulent kinetic energy, temperature, and species concentration variances can be estimated from high-frequency fluctuations of these quantities in the inertial subrange. The latter is the frequency range between the large-scale eddies that create most of the turbulent fluctuations and the smallest eddies that dissipate the variance through molecular diffusion. The standard deviation of the fluctuations in this intermediate frequency range is proportional to the dissipation to the 1/3 power. By making concurrent measurements of the velocity, temperature, and species concentration fluctuations in the inertial subrange it is possible, through consideration of the variance budgets of these variables, to simultaneously estimate the fluxes of these quantities (*37, 38*). This technique is particularly well suited for ship measurements (*39*) because it is not necessary to make corrections for ship motions, and the measurements are less affected than covariance measurements by flow distortion caused by the ship and supporting structures.

Budget techniques. A different approach for estimating surface flux is through the use of ambient mass balance or budget techniques. In contrast to variance and profile techniques, these are absolute techniques in that empirical relations are unnecessary to estimate the flux. The basis for this method is to evaluate the various terms that can change the mean concentration of a species with time [see, for example, (*1*)]. One approach is to integrate these terms over a reference volume or box. As discussed by Williams (*40*), often it is difficult to obtain sufficiently accurate concentration differences between the upwind and downwind planes of the box. Mass balance

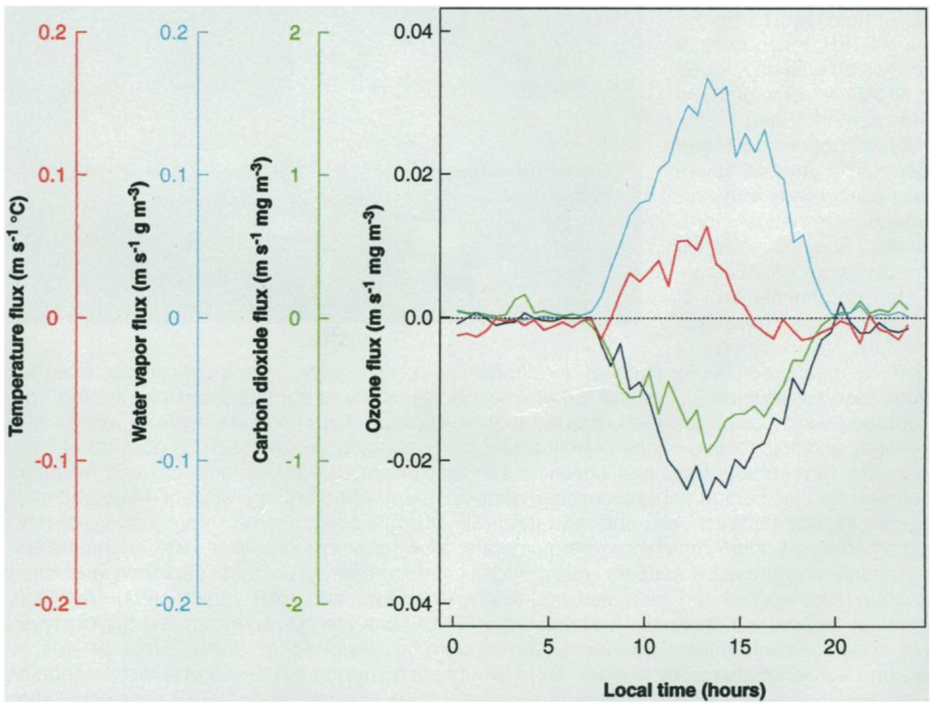

Fig. 3. Fluxes of sensible heat, water vapor, carbon dioxide, and ozone measured over an irrigated cotton field measured with the eddy-correlation technique as part of the San Joaquin Valley Air Quality Study. These data shown were taken on 26 July 1992 at a height of 5 m above ground. At sunrise (0700 local time), the cotton plants begin photosynthesis, consuming CO_2 as seen by the negative flux (air to ground). Stomates on the plant leaves must open to allow CO_2 to exchange with the atmosphere, and so water (taken up by roots from the soil) can leave the plant, which causes a positive flux (ground to air). Ozone also is consumed by the cotton. Photosynthesis on this day appeared limited only by solar radiation, which caused fluxes to peak at noon and drop off in the afternoon. The small positive CO_2 flux at night is evidence of respiration, when the plans consume O_3 and release CO_2. During morning, some solar energy is available for heating the ground after most has been used to evaporate the water, so heat is transferred from the ground to the air and a positive sensible heat flux is observed. By mid-afternoon, air near the ground cools rapidly because of evaporation, so the overlying air is warmer and heat is transferred downward.

approaches have also been applied to estimating surface flux from treated (for example, fertilized) plots of limited along-wind extent [see, for example, (*34, 35, 41*)] and motor vehicle emissions in urban areas (*42, 43*). This approach permits evaluation of the surface flux from measurements of mean concentration and horizontal wind as a function of height downwind of the test area. However, stability affects the height to which the emission plume extends and over which measurements must be made. In Fig. 4, surface flux estimates of sensible and latent heat obtained by the energy budget technique are compared with those of three other techniques: eddy correlation, profile, and conditional sampling.

Enclosure techniques. Enclosures serve as a bridge between laboratory process studies and ambient flux studies. Enclosures are usually chambers that are placed over ground, water, or vegetation; fluxes are derived from the rate of change in concentration. They are simple, relatively inexpensive, and robust, and allow the measurement of base emission rates of specific ecosystem components. Enclosures also allow quick exploration of the range and types of emissions that can occur in specific ecosystems. For example, enclosures allow the isolation of specific trace gas sources and the collection of samples that are adequate for gas chromatographic–mass spectrometric analyses of composition and determination of isotopic fingerprints. In addition, chamber measurements enable monitoring of emissions over very long periods. Chambers are best for investigating questions related to spatial scales that range from organisms to leaves to plants, isolation of specific emission processes, and identification of source variability within ecosystems. Despite precautions, chamber studies always suffer from uncertainty due to disturbances during the enclosure period. These disturbances range from damage to fragile terpene-containing structures in some leaves, to the effects of bubbles and vegetation mats in wetland studies of methane production, to suppression of atmospheric flow and turbulence.

Enclosures are used mainly to sample individual leaves, branches, and sometimes whole trees, as well as ground and water surfaces. Enclosure deployment and interpretation of the measurements require extremely detailed information about ecosystem structure. For example, to estimate the isoprene flux from an ecosystem by using enclosure data, the vegetation species composition and leaf biomass for each species must be known. In addition, corrections must be made for the departure from the average ecosystem temperature and for light and canopy-structure effects; enclosures can also be constructed to have some degree of environmental control. Enclosure data can be obtained for most temperate ecosystems, but enclosure technology has severe limitations in much of the tropics where species diversity is high and the top of the canopy is often difficult to reach. Furthermore, chambers cannot entirely address questions of site representativeness. For many trace gases, a small percent of the research area can account for most of the emissions. Important components of the emissions may be omitted with inadequate numbers or improper siting of enclosures.

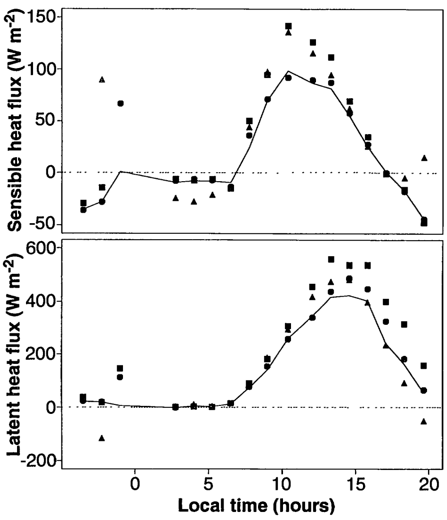

Fig. 4. A comparison between sensible and latent heat fluxes measured by four techniques. The measurements were obtained 25 July 1991 in the San Joaquin Valley of California over an irrigated cotton field. Eddy-correlation measurements (solid lines) were made 5 m above ground. The flux-profile technique (filled squares) was applied by using differences between average temperature and humidity measurements at heights of 3 and 7.5 m. The Bowen ratio–energy balance method (filled triangles) used net radiometer data 3 m above ground, temperature and humidity differences between 3 and 7.5 m, and soil heat flux measurements at a depth of 8 cm. Conditional sampling (filled octagons) was simulated from the fast-response temperature and humidity measurements. All four techniques agree to within 100 W m^{-2} most of the time and often to within 20 W m^{-2}. The conditional sampling technique compares most favorably with the reference with differences typically <19 W m^{-2}. The flux profile estimates have biases in sensible heat flux of ~20 W m^{-2} and in latent heat of ~100 W m^{-2}. The Bowen ratio–energy budget yields fluxes that are generally <40 W m^{-2} with occasional larger errors. In this comparison, all of the large errors occur during the evening when the temperature and humidity measurements used to partition the available energy into sensible and latent heat are sensitive to small calibration errors.

Measurement Issues and Considerations

Many important considerations must be addressed to make accurate measurements of turbulent fluxes. These considerations are particularly important for eddy correlation and can include frequency response of wind and scalar sensors, averaging interval for processing time series, measurement height, homogeneity and representativeness of the measurement site, and flow distortion by the instrumentation. Often these criteria impose conflicting requirements. In the early days of micrometeorology, rules of thumb were developed to provide practical guidance; many of these issues are currently being addressed in an increasingly detailed and quantitative manner. Recent detailed reviews are found in Businger (*28*), Baldocchi *et al.* (*44*), Fowler and Duyzer (*35*), Wyngaard (*45*), Kaimal and Finnigan (*3*), and Lenschow (*9*).

Surface-exchange measurements can be made from towers or aircraft. Advantages of aircraft measurements are that true spatially averaged fluxes can be made over surfaces that are difficult to access from the ground, such as forests and oceans, and that averaging times are reduced because airplanes travel about an order of magnitude faster than the mean wind. However, airborne flux estimates must be extrapolated to the surface, and aircraft motions must be removed from the measured air velocity before velocity fluctuations relative to the earth can be obtained. The relatively faster air velocity also means that corrections for compressibility of the air, which scale with the square of the air speed, are important. On the other hand, tower-based measurements can be made continuously and are more representative of true surface fluxes.

Vertical advection. The total vertical flux of any species has contributions from two terms, an advection term that is the product of the average vertical velocity and the average species concentration, and an eddy flux term that is the flux measured by eddy correlation, gradient transfer, and so forth. The advection term is often neglected with the assumption that the average vertical velocity is zero at or near the surface. Webb *et al.* (*46*) point out that the proper assumption is that the vertical flux of dry air is zero at the surface. As a consequence, there is a small nonzero average vertical velocity equal to the negative of the eddy density flux divided by the density of dry air, where the eddy density flux has contributions from the sensible heat and water vapor fluxes. The resulting correction to the species eddy flux is only significant when the deposition velocity is less than 1 cm s^{-1}. This so-called Webb correction applies to fluxes determined by vertical gradient measurements as well as eddy correlation measurements. The contribution of the advection term to the total flux is zero if, instead of measuring the species density, mixing ratio with respect to dry air is measured. Lenschow (9) notes two ways to implement the latter approach: (i) preprocess the air by drying and adjusting to a constant temperature and pressure prior to measuring the species density, or (ii) measure the ratio of the species density to the density of a second species that is uniformly mixed, such as N_2 or O_2. Finally, if the mixing ratio with respect to total air density is measured, then the measured flux need only be corrected for water vapor flux, which is typically several times smaller than the correction for sensible heat flux.

Averaging time. Eddy fluxes are effected by a broad range of eddy sizes that must be adequately sampled by choosing proper averaging times and sensor frequency response to determine accurately the flux by eddy correlation. Lenschow *et al.* (*47*) distinguish between systematic errors caused by nonrepresentative sampling of large eddies and random errors associated with a finite number of independent samples. They conclude that for averaging times much greater than the integral time scale of the turbulent transport process, the systematic error becomes small and much less than the random error. (One situation where the systematic error may be relevant is the measurement of a scalar flux by an aircraft passing repeatedly over a limited area.) Lenschow and Kristensen (*48*) found that the fractional random flux measurement error is proportional to the square root of the ratio of the integral length scale to the sample length and inversely proportional to the correlation coefficient between vertical velocity and species concentration. For a wind speed of 5 m s^{-1} at a measurement height of 10 m, the required averaging time is ≥ 20 min for a fractional error $<20\%$; reducing that error to 10% requires averaging four times longer. For aircraft measurements at a height of 50 m in a 1000-m-deep CBL, the same 20% error limit requires a flight leg on the order of 30 km.

Stationarity. Reduction of the random sampling error by increasing the averaging time is usually in conflict with the requirement for stationarity. A process is stationary when its statistical properties are independent of time, and thus stationarity permits the calculation of averages that represent properties of the process and not those of the averaging period. However, the basic diurnal cycle and the passage of weather systems usually limit stationary periods to 1 hour or less. The effects of underlying nonstationary processes on the average are often reduced by removing an identified trend from the data or by high-pass filtering of the data (*47*).

Sensor response. The required sampling rate and sensor frequency response are defined by the high-frequency tail of the flux cospectrum. Schmitt *et al.* (*49*) show that flux cospectra for scalars are similar when nondimensionalized with appropriate scaling parameters. In the unstable to neutral SL, "universal" cospectra may be determined by scaling the wavelength $\bar{u}/f$ with z, where f is frequency and $\bar{u}$ is the wind speed (airspeed in the case of aircraft measurements) at the measurement height. For stable stratification, z diminishes in importance as stability increases and the scaling length becomes dependent on L (*50*). In the CBL, the appropriate scaling length is z_i (*51*). For the two preceding examples, frequency response should extend to ~2 Hz, but aircraft measurements in the SL require ~10-Hz response.

Measurement height. Tower-based measurements often involve a conflict between requirements for sensor height and site homogeneity. Since turbulent eddies generally scale with height in the SL, the frequency response of the wind and scalar sensors used for eddy correlation will determine the minimum height (often ≥ 5 to 10 m) where the smallest eddies affecting vertical transport can be sampled adequately. Species concentration profiles scale with the logarithm of height; measurement heights should ideally differ by a factor of ≥ 10 to accurately resolve vertical gradients. As a consequence, micrometeorological flux measurements are effectively averaged over an extended upwind area. This approach has the advantage of providing a surface flux measurement that is integrated over small-scale variations in surface composition.

Site homogeneity. The areal "footprint" seen by tower-mounted flux sensors must be homogeneous on the large scale to avoid horizontal advection and thus vertical flux divergence that causes the measured flux to differ from the surface flux of interest. [Vertical flux divergence can also be caused by near-surface sources or sinks of a reactive chemical species (*10*) or by an entrainment flux at the top of a CBL that is much larger than the surface flux (*28*).] Leclerc and Thurtell (*52*), Schuepp *et al.* (*53*), and Horst and Weil (*54, 55*) used theoretical models of the flux footprint to determine the required fetch. They find that stably stratified conditions require much greater fetches than unstable conditions, and the fetch required for even moderately stable conditions is for many situations considerably greater than 100 times the measurement height, which is the conventional rule.

Vertical alignment. The measurement of a vertical flux by eddy correlation requires careful physical alignment of the vertical velocity sensor in the field and analytical rotation of the coordinate axes during postprocessing of the data. This is necessary to avoid contamination of the vertical flux measurement by the streamwise flux, which is opposite in sign to the vertical flux and can be as much as three times greater (*56*). The anemometer is best aligned in the field with respect to gravitational vertical, but this is adequate by itself only over flat, homogeneous terrain. If the mean flow field is not horizontal, both the horizontal and vertical components of the flux should be measured with a three-component anemometer and the measured fluxes should be analytically rotated to a coordinate system with axes parallel and normal to the streamlines.

For aircraft measurements, the velocity and attitude angles of the airplane relative to the earth are commonly obtained from an inertial navigation system, which contains an orthogonal triad of accelerometers whose outputs are integrated to obtain airplane velocity and position. The accelerometers may be mounted either on a gyrostabilized platform or mounted directly to the aircraft, with local earth vertical and true north updated continuously by means of computer calculations. The air velocity relative to the aircraft must be rotated to the local earth coordinate system to calculate the three wind components in an earth-based frame of reference [see (*57*)].

Flow distortion. Contamination of the measured vertical flux by the streamwise flux can also be caused by flow distortion around the sensors and supporting structures. To avoid cross talk, the sensor array should be symmetric about the horizontal plane passing through the point at which the vertical velocity is measured. Even in a symmetric array, the vertical velocity is amplified and the flux is overestimated by blockage of the flow (*58*). The bulk of the array should be minimized so that vertical velocity is measured at a point where the stagnation loss in streamwise wind speed is minimal.

Wyngaard (*59*) finds that scalar density and density flux can also be altered by flow distortion. At typical aircraft speeds, the scalar density flux can be contaminated by sensible heat and momentum fluxes, while the mixing ratio flux is conserved. The obvious remedies are to minimize flow distortion and to measure mixing ratio rather than density, as already recommended to eliminate the need for the Webb correction. Even for conserved quantities such as the mixing ratio, the scalar time series is unaltered by flow distortion only if $(q/\bar{u})(a/l)^{1/3} << 1$, where a is a characteristic dimension of the bluff body and q and l are characteristic velocity and length scales of the turbulence. This requirement is easily satisfied at aircraft speeds and is more difficult, but not impossible, to achieve for tower measurements.

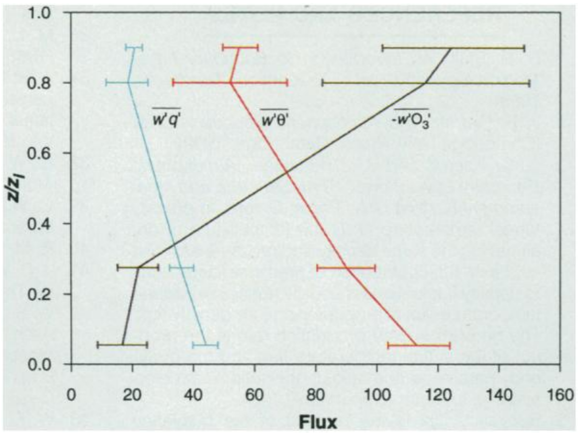

Fig. 5. Over-water boundary-layer mean flux profiles of potential temperature [θ (m s^{-1} mK)], water vapor (m s^{-1} mg m^{-3}), and ozone (m s^{-1} mg m^{-3}) [adapted from Kawa and Pearson (76)] from Flight 5 of the summer 1985 DYCOMS experiment off the central California coast. Fluxes were determined by the eddy-correlation technique from 20-Hz measurements from the NCAR Electra aircraft along a 23.6-km track. Error bars represent 90% confidence limits on the mean fluxes. Positive fluxes are defined here to be away from the ocean surface; the flux-profile structure is indicative of the ocean surface as a source of heat and water vapor and a sink for ozone.

Sonic anemometers. Turbulence-scale velocity measurements in the SL are most commonly made with sonic anemometers. These measure a component of the wind velocity by detecting the difference in transit times of acoustic pulses propagating in opposite directions across a known path; three individual paths are required to measure all wind components. Their advantages are rapid response, linear output, and stable calibration, but their principal drawback is high cost. Hot wire or hot film anemometers provide higher frequency response but are fragile and susceptible to calibration shifts. Mechanical anemometers are rugged and less expensive, but usually have marginal frequency response for eddy correlation. Dynamic anemometers, such as pressure spheres, can be built with a frequency response that is adequate for flux measurements, but such instruments are insensitive to low wind speeds and usually must be custom-made and calibrated.

The principal limit to the sonic anemometer frequency response is imposed by line averaging along the measurement path. Its response is degraded for wavelengths less than $2\pi d$, where d is the path length, typically 10 to 20 cm. For general turbulence measurements, this dictates a minimum measurement height of 25 times the path length (60), but Kristensen and Fitzjarrald (61) have shown that for scalar fluxes this criterion can be relaxed to five times the path length. They caution, however, that measuring scalar fluxes at heights of 1 m or less may introduce problems associated with nonrepresentative sampling of small-scale surface inhomogeneities.

Recent work has focused on disturbance of the flow field by the sensor array. Kaimal and Gaynor (62) note that a correction must be made to the measured wind component for the velocity deficit in the transducer wake ("transducer shadow"). Wyngaard (63) examined in detail the implications for turbulence measurements of flow distortion induced by the entire sensor array. Zhang *et al.* (64) and Kaimal *et al.* (65) describe recent sonic anemometer probe geometries designed to minimize flow distortion by the sensor.

Aircraft measurements. Air velocity relative to the aircraft is commonly measured by a combination of instruments. A Pitot tube mounted at the front of the aircraft is used, along with a static pressure port, for a pressure difference measurement which is called the dynamic pressure. This measurement is combined with static pressure and air temperature to obtain the true airspeed (the magnitude of the air velocity vector). This measurement is then combined with a measurement of the air flow angles of the velocity vector (using vanes or differential pressure measurements) relative to the longitudinal axis of the airplane.

Although aircraft have been used to measure fluxes at levels <30 m above the surface (66), they often, for safety reasons, are not flown close enough to the surface to measure the surface flux directly. Surface fluxes can be obtained by flying at several levels and linearly extrapolating the flux profile to the surface, since for conserved species in a horizontally homogeneous and well-mixed boundary layer the flux varies linearly with height (47). An example of overwater aircraft flux measurements of temperature, water vapor, and ozone is shown in Fig. 5.

Air sampling. Chemical analyzers used for eddy correlation measurements of trace gas fluxes are often located some distance away from the sampling point, which must be near the anemometer. Transport of the sampled air to the analyzer through tubing introduces both a time lag and high-frequency attenuation of the concentration fluctuations. Lenschow and Raupach (67) provide estimates of the frequency-dependent attenuation, caused by longitudinal and lateral diffusion within the tubing, and show that the attenuation is minimized when the flow within the tubing is fast enough to be turbulent.

Enclosures. A wide range of chamber technologies has been developed for measuring fluxes from soils, surface water, and trees. They range from simple bags and cans (68) to temperature- and light-controlled cuvettes (69). Usually there is a direct relation between simplicity, portability, numbers of samplers, and logistic requirements. Simple systems are most suitable for exploratory and survey work. Carefully controlled systems are required to isolate variables and to develop algorithms.

Materials used in chambers vary depending on the trace gas flux of interest. Teflon film is often used in experiments to determine biogenic nonmethane hydrocarbon emissions from vegetation. It is inert, has a low rate of out-gassing, and is transparent at photosynthetically active wavelengths. Simple nonregulated enclosures can only be used for short time periods (typically 2 to 5 min) in sunlight without overheating problems (68). Nontransparent materials such as stainless steel can be used for trace gases such as methane and nitrous oxide, where radiation effects are unimportant.

Rigid enclosures require pressure equilibration (70). This is usually accomplished with a long capillary vent tube or a flexible plenum. Flexible bag enclosures require accurate estimation of the internal volume. This can be accomplished by adding a known quantity of an easily detected tracer (such as sulfur hexafluoride or butane) and using the dilution factor to calculate the volume (71). Some enclosures are static and have no provision for mixing air thoroughly. Most incorporate either an internal fan or use a gas pump to recirculate air and minimize potential SL effects.

Dynamic or flow-through chambers use air of a known composition to continually sweep the chamber volume. The flow rate must be accurately known, but the chamber volume is not critical for accurate flux determination. These systems also have the advantage of mitigating temperature increases by continual flushing. High flow rates place greater demands on analytical sensitivity and precision and require precise control of the composition of the flush air.

Some portable cuvette systems independently control temperature, CO_2, sunlight, and humidity. These systems have been used to develop canopy-specific flux algorithms in the field. Previously used to measure CO_2 fluxes, they recently have been adapted to isoprene flux estimates in the field.

Summary

Both the measurement and modeling of surface fluxes are difficult owing to the complexity of the source and sink mechanisms, the significant heterogeneity of the earth's land surface, the role of atmospheric turbulence in controlling the rate of exchange between the earth's SL and ABL, and the inherent limitations of the various measurement techniques. Conventional enclosure techniques offer the advantage of providing plant- or leaf-specific measurements, yet these are limited by their lack of spatial representativeness and the modification of the local environment by the enclosure. Micrometeorological techniques can provide accurate flux estimates, but have relatively large personnel demands and sophisticated instrumentation and data-processing requirements. Perhaps a reasonable compromise for ground-based measurements may be obtained through the application of automated conditional sampling techniques (which are under development); conditional sampling results to date are encouraging but not yet definitive. Similar consideration must be given to trade-offs between surface-based and airborne measurements. The former are more easily obtained but frequently are limited in their spatial representativeness and ideally require flat sites with homogeneous source-sink characteristics. Airborne flux measurements are spatially representative but are more difficult and do not provide good temporal resolution or continuity.

For the foreseeable future, air-surface exchange measurements will continue to require careful and judicious selection of in situ measurement techniques that have the appropriate impedance match to the problem at hand. In principle, active remote sensors offer the potential to provide vertical flux profiles through the ABL although most current efforts are directed at obtaining reliable concentration profiles (*72*). Relatively fast Doppler and interferometric wind profilers have demonstrated the feasibility of profiling momentum flux (*73*) by variance and eddy-correlation techniques; efforts are also underway to estimate the heat flux by combining wind profiling and radio acoustic sounding technologies. As challenging as these efforts are, others are seeking to develop remote sensors that can obtain vertical profiles of trace-gas fluxes (particularly for H_2O, O_3, and SO_2). Several flux-analysis methods are potentially applicable; these include eddy correlation, flux-profile relations, dissipation (*74*), and conditional sampling. Remote gas-flux profile measurements can only be expected to be feasible in the CBL because of instrumental range-resolution limitations and dwell-time requirements, and larger daytime flux magnitudes. Considerable additional research and testing is required before reliable remote sensing of flux profiles is a reality—a worthy goal not likely to be achieved in the near future.

REFERENCES AND NOTES

1. R. B. Stull, *An Introduction to Boundary Layer Meteorology* (Kluwer Academic, Dordrecht, 1988).
2. J. R. Garratt, *The Atmospheric Boundary Layer* (Cambridge Univ. Press, Cambridge, 1992).
3. J. C. Kaimal and J. J. Finnigan, *Atmospheric Boundary Layer Flows—Their Structure and Measurement* (Oxford Univ. Press, Oxford, in press).
4. Virtual temperature (θ) is the temperature of dry air having the same density and pressure as moist air. Since the contribution of pressure fluctuations to density fluctuations is usually negligible, virtual-temperature flux is proportional to air density flux. The buoyant energy production rate is the product of the virtual temperature flux and the buoyancy parameter (the ratio of gravitational acceleration, *g*, to mean temperature).
5. Buoyancy flux is the product of the buoyancy parameter and the flux of virtual temperature.
6. J. C. Wyngaard and R. A. Brost, *J. Atmos. Sci.* **41**, 102 (1984).
7. C.-H. Moeng and J. C. Wyngaard, *ibid.*, p. 3161.
8. ——, *ibid.* **46**, 2311 (1989).
9. D. H. Lenschow, in *Methods in Ecology: Trace Gases*, P. Matson and R. Harriss, Eds. (Blackwell, Cambridge, MA, in press).
10. D. R. Fitzjarrald and D. H. Lenschow, *Atmos. Environ.* **17**, 2505 (1983).
11. D. H. Lenschow and A. C. Delany, *J. Atmos. Chem.* **5**, 301 (1987).
12. G. Kramm *et al.*, *ibid.* **13**, 265 (1991).
13. S. J. Caughey, J. C. Wyngaard, J. C. Kaimal, *J. Atmos. Sci.* **6**, 1041 (1979).
14. J. Kim and L. Mahrt, *Tellus* **44A**, 381 (1992).
15. W. A. Cooper, unpublished results.
16. R. L. Desjardins, thesis, Cornell University, Ithaca, NY (1972).
17. B. B. Hicks and R. T. McMillen, *J. Clim. Appl. Meteorol.* **23**, 637 (1984).
18. J. A. Businger and S. P. Oncley, *J. Atmos. Oceanic Technol.* **7**, 349 (1990).
19. J. C. Wyngaard and C.-H. Moeng, *Boundary-Layer Meteorol.* **60**, 1 (1992).
20. J. M. Baker, J. M. Norman, W. L. Bland, *Agric. Forest Meteorol.* **62**, 31 (1992).
21. S. P. Oncley, A. C. Delany, T. W. Horst, P. P. Tans, *Atmos. Environ.*, in press.
22. E. Pattey, R. L. Desjardins, P. Rochette, *Boundary-Layer Meteorol.*, in press.
23. S. D. Smith, *J. Geophys. Res.* **93**, 15,467 (1988); *ibid.*, p. 15,472.
24. P. S. Liss, in *Air-Sea Exchange of Gases and Particles*, P. S. Liss and W. G. N. Slinn, Eds. (Reidel, Dordrecht, 1983), pp. 241–298.
25. —— and L. Merlivat, in *The Role of Air-Sea Exchange in Geochemical Cycling*, P. Buat-Ménard, Ed. (Reidel, Dordrecht, 1986), pp. 113–127.
26. P. S. Liss and P. G. Slater, *Nature* **247**, 181 (1974).
27. M. L. Wesely, *Trace Atmospheric Constituents: Properties, Transformations, and Fates*, S. E. Schwartz, Ed. (Wiley, New York, 1983), pp. 346–370.
28. J. A. Businger, *J. Clim. Appl. Meteorol.* **25**, 1100 (1986).
29. K. J. Davis, thesis, University of Colorado, Boulder (1992).
30. M. R. Raupach, in *Flow and Transport in the Natural Environment: Advances and Applications*, W. L. Steffen and O. T. Denmead, Eds. (Springer-Verlag, Berlin, 1988), pp. 95–127.
31. ——, J. J. Finnigan, Y. Brunet, paper presented at the Fourth Australasian Conference on Heat and Mass Transfer, Christchurch, New Zealand, 9 to 12 May 1989.
32. W. J. Shuttleworth, *Philos. Trans. R. Soc. London Ser. B* **324**, 299 (1989).
33. P. Cellier and Y. Brunet, *J. Agric. Forest Meteorol.* **58**, 93 (1992).
34. O. T. Denmead, in *Gaseous Loss of Nitrogen from Plant-Soil Systems*, J. R. Freney and J. R. Simpson, Eds. (Nijhoff/Junk, The Hague, 1983), pp. 133–157.
35. D. Fowler and J. H. Duyzer, in *Exchange of Trace Gases between Terrestrial Ecosystems and the Atmosphere*, M. O. Andreae and D. S. Schimel, Eds. (Wiley, New York, 1989), pp. 189–207.
36. M. L. Wesely, *Boundary-Layer Meteorol.* **44**, 13 (1988).
37. J. B. Edson, C. W. Fairall, P. G. Mestayer, S. E. Larsen, *NOAA Tech. Memor. ERL WPL-199* (National Technical Information Service, Springfield, VA, 1991).
38. C. W. Fairall and S. E. Larsen, *Boundary-Layer Meteorol.* **34**, 287 (1986).
39. C. W. Fairall, J. B. Edson, P. G. Mestayer, S. E. Larson, *J. Atmos. Oceanic Technol.* **7**, 425 (1990).
40. R. M. Williams, *Atmos. Environ.* **16**, 2707 (1982).
41. J. D. Wilson, V. R. Catchpole, O. T. Denmead, G. W. Thurtell, *Agric. Meteorol.* **29**, 283 (1983).
42. W. B. Johnson, F. L. Ludwig, W. F. Dabberdt, R. J. Allen, paper presented at the Sixty-fourth Annual Meeting of the American Institute of Chemical Engineers, San Francisco, 28 November to 2 December 1971.
43. W. F. Dabberdt and R. N. Dietz, in *Probing the Atmospheric Boundary Layer*, D. Lenschow, Ed. [American Meteorological Society (AMS), Boston, MA, 1986], pp. 103–121.
44. D. D. Baldocchi, B. B. Hicks, T. P. Meyers, *Ecology* **69**, 1331 (1988).
45. J. C. Wyngaard, *Boundary-Layer Meteorol.* **50**, 49 (1990).
46. E. K. Webb, G. I. Pearman, R. Leuning, *Q. J. R. Meteorol. Soc.* **106**, 85 (1980).
47. D. H. Lenschow, J. Mann, L. Kristensen, unpublished results.
48. D. H. Lenschow and L. Kristensen, *J. Atmos. Ocean Technol.* **2**, 68 (1985).
49. K. F. Schmitt, C. A. Friehe, C. H. Gibson, *J. Atmos. Sci.* **36**, 602 (1979).
50. J. C. Kaimal, J. C. Wyngaard, Y. Izumi, O. R. Coté, *Q. J. R. Meteorol. Soc.* **98**, 563 (1972).
51. D. H. Lenschow and B. B. Stankov, *J. Atmos. Sci.* **43**, 1198 (1986).
52. M. Y. Leclerc and G. W. Thurtell, *Boundary-Layer Meteorol.* **52**, 247 (1990).
53. P. H. Schuepp, M. Y. Leclerc, J. I. Macpherson, R. L. Desjardins, *ibid.* **50**, 355 (1990).
54. T. W. Horst and J. C. Weil, *ibid.* **59**, 279 (1992).
55. ——, unpublished results.
56. J. C. Wyngaard, O. R. Coté, Y. Izumi, *J. Atmos. Sci.* **28**, 1171 (1971).
57. D. H. Lenschow, in *Probing the Atmospheric Boundary Layer*, D. H. Lenschow, Ed. (AMS, Boston, 1986), pp. 29–55.
58. J. C. Wyngaard, *Boundary-Layer Meteorol.* **42**, 19 (1988).
59. ——, *J. Atmos. Sci.* **45**, 3400 (1988).
60. J. C. Kaimal, in *Probing the Atmospheric Boundary Layer*, D. H. Lenschow, Ed. (AMS, Boston, 1986), pp. 19–28.
61. L. Kristensen and D. R. Fitzjarrald, *J. Atmos. Oceanic Technol.* **1**, 138 (1984).
62. J. C. Kaimal and J. E. Gaynor, *J. Appl. Meteorol.* **22**, 863 (1983).
63. J. C. Wyngaard, *ibid.* **20**, 784 (1981).
64. S. F. Zhang, J. C. Wyngaard, J. A. Businger, S. P. Oncley, *J. Atmos. Ocean Technol.* **2**, 548 (1986).
65. J. C. Kaimal, J. E. Gaynor, H. A. Zimmerman, G. A. Zimmerman, *Boundary-Layer Meteorol.* **53**, 103 (1990).
66. R. L. Desjardins and J. I. MacPherson, in *Exchange of Trace Gases between Terrestrial Ecosystems and the Atmosphere*, M. O. Andreae and D. S. Schimel, Eds. (Wiley, New York, 1989), pp. 135–152.
67. D. H. Lenschow and M. R. Raupach, *J. Geophys. Res.* **96**, 15,259 (1991); *ibid.*, p. 15,268.
68. P. Zimmerman, *EPA Rep. 450-4-70-004* (U.S. Environmental Protection Agency, Research Triangle Park, NC, 1979).
69. A. Guenther, R. Monson, R. Fall, *J. Geophys. Res.* **97(D6)**, 10799 (1991).
70. R. Cicerone, C. Delwiche, S. Tyler, P. Zimmerman, *Global Bio. Cycles* **6**, 233 (1992).
71. L. Klinger, P. Zimmerman, J. Greenberg, L. Heidt, A. Guenther, *J. Geophys. Res.*, in press.
72. *Optical Remote Sensing of the Atmosphere Technical Digest* (Optical Society of America, Washington, DC, 1993); *Proceedings of the Second International Tropospheric Profiling Symposium*

(NCAR, Boulder, CO, 1991); R. L. Schwiesow, in *Probing the Atmospheric Boundary Layer*, D. Lenschow, Ed. (AMS, Boston, 1986), pp. 139–162. W. B. Grant, *Opt. Eng.* **30**, 40 (January 1991). D. I. Cooper *et al.*, *Boundary-Layer Meteorol.* **61**, 389 (1992).
73. *Proceedings of 5th SCOSTEP/URSI Workshop on Technical and Scientific Aspects of MST Radar*, (SCOSTEP Secretariat, University of Illinois, Urbana, IL 61801, 1991).
74. W. E. Eichinger *et al.*, *Boundary-Layer Meteorol.* **63**, 39 (1993).
75. J. A. Businger, W. F. Dabberdt, A. C. Delany, T. W. Hors, C. L. Martin, S. P. Oncley, S. R. Semmer, *Bull. Am. Meteor. Soc.* **71**, 1006 (1990). ASTER is supported by NCAR for the general use of the scientific community. Scientists, engineers, and technicians provide field and laboratory support. NCAR also provides the community with aircraft instrumented for flux (and other) measurements. User scientists design the field experiments, frequently bring additional instrumentation to the facilities, and are responsible for the scientific analysis and interpretation of the data. Applications for ASTER and aircraft field support should be directed to the Managers of NCAR's Surface & Sounding Systems Facility and Research Aviation Facility, respectively. A community peer-review panel meets semiannually to advise NCAR and the National Science Foundation on the requests. The computational facility is based on a server/workstation architecture. The Sun 4/280 server provides the major disk storage (1.96 gigabytes) and computational capability for data collection and routine processing. Additional workstations allow for ancillary calculations and high-resolution color graphics displays. A tape drive provides high-density data backup.
76. S. R. Kawa and R. Pearson, Jr., *J. Atmos. Sci.* **46**, 2649 (1989).
77. NCAR is sponsored by the National Science Foundation.